Self-calibrating finite-volume schemes for unstructured grids

M. Bernard[1], G. Lartigue[2], G. Balarac[1], and V. Moureau[2]

[1]LEGI, CNRS UMR 5519, Grenoble-INP, Université de Grenoble, Saint Martin d'Hères, France
[2]CORIA, CNRS UMR-6614, INSA de Rouen, Université de Rouen, Saint-Etienne-du-Rouvray, France

Extrem CFD Workshop, Toulouse, July 2017

The aim of this study is to devise a new numerical scheme that will ensure a given spatial convergence order on unstructured grids with highly distorted elements. Indeed, the spatial discretisation of a transport equation can be of high order on regular meshes but will fall to low order while grid's regularity gets worse. Unfortunately, many geometrical configurations request unstructured meshes, *i.e.* containing cells of high and/or various aspect ratios, or even a mix of different cell types (for example, prisms and tetrahedrons). Different techniques have been proposed over years to ensure the desired precision of solution (for example, k-exact method [**?**, **?**, **?**, **?**]). The present study tries to extend these methods into a novel direction by designing a self-calibrating scheme family.

The first step of the method presented here consists in the correction of discretisation errors that appears on the gradient and hessian operators on a given location I.

$$\begin{pmatrix} G_I^{\mathcal{O}2} \\ H_I^{\mathcal{O}1} \end{pmatrix} = \left(\underline{\underline{D}}_I^{\mathcal{O}3}\right) \cdot \begin{pmatrix} \mathcal{G}_I \\ \mathcal{H}_I \end{pmatrix} \tag{1}$$

Where $\mathcal{G}_I$ and $\mathcal{H}_I$ are the discrete Gradient and Hessian operators applied to any tensorial field T, respectively. $G_I^{\mathcal{O}2}$ and $H_I^{\mathcal{O}1}$ are the Gradient and Hessian operators corrected at order 2 and 1, respectively. $D_I^{\mathcal{O}3}$ is the deconvolution matrix that must be evaluated once for all at each mesh location I during a pre-processing step: it combines both the mesh quality and the properties of the discrete operators but will not evolve in time.

The second step is the deconvolution at each node of the quantity averaged over the associated control volume (dual mesh):

$$T_I^{\mathcal{O}3} = \overline{T}^I - \overline{\mathbf{\Delta}_I}^I \cdot G_I^{\mathcal{O}2} - \frac{1}{2}\left(\overline{\mathbf{\Delta}_I \otimes \mathbf{\Delta}_I}^I\right) : H_I^{\mathcal{O}1} + \mathcal{O}(\Delta^3) \tag{2}$$

Where $\overline{\mathbf{\Delta}_p}^p$ and $\overline{\mathbf{\Delta}_p \otimes \mathbf{\Delta}_p}^p$ are the first and second order moments of the control volume, respectively.

The third step is the reconstruction of the solution around the point I:

$$T^{\mathcal{O}3}(\mathbf{x}) = T_I^{\mathcal{O}3} + (\mathbf{x} - \mathbf{x}_I) \cdot G_I^{\mathcal{O}2} + \frac{1}{2}\Big((\mathbf{x} - \mathbf{x}_I) \otimes (\mathbf{x} - \mathbf{x}_I)\Big) : H_I^{\mathcal{O}1} + \mathcal{O}(\Delta^3) \tag{3}$$

Finally, in a last step, it is the possible to integrate this polynomial exactly on control-volume interfaces to compute the numerical flux associated to this reconstruction. Several flux reconstruction can be used on a single interface to create a variety of numerical schemes (centered, upwind, weno, ...) but this aspect has not been covered during the workshop.

For now, the method is implemented in YALES2 for scalar convection only but extension to Navier-Stokes equations should not be a major problem. Both 1D and 2D implementation where already finished at the beginning of the workshop. The Fig. 1 shows the spatial convergence of the method on a 2D mesh fully composed of triangles, the domain being periodic in both directions. The test-function is $C^\infty$and has a compact support and the error is measured after 1 period. One can see that the classical "4^{th} order" space integration scheme degenerates to order 1.5 for highly distorted mesh. On the other hand, the 3rd order self-calibrating method ensures the expected convergence, regardless of the mesh regularity.

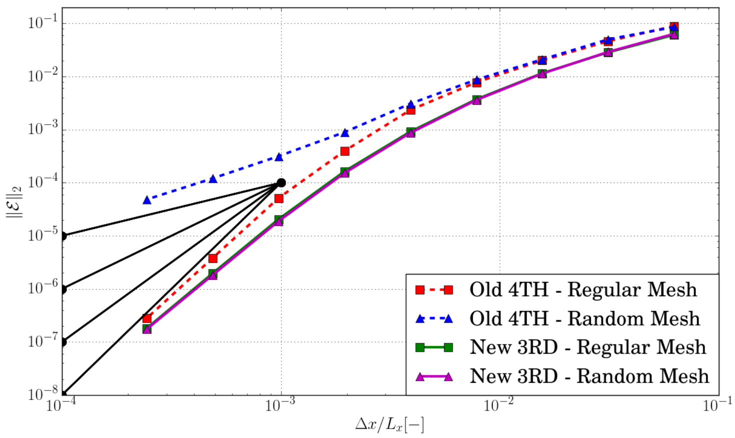

Figure 1: 2D - Spatial convergence for a bump function transported through a bi-periodic domain

During this workshop, we focused on the extension of the method to 3D, with both 2^{nd} and 3^{rd} order reconstruction. We succeed in implementing and testing the 2^{nd} order scheme as one can see on Fig. 2. Indeed, here again, the expected order is ensured with the new scheme on distorted meshes whereas it

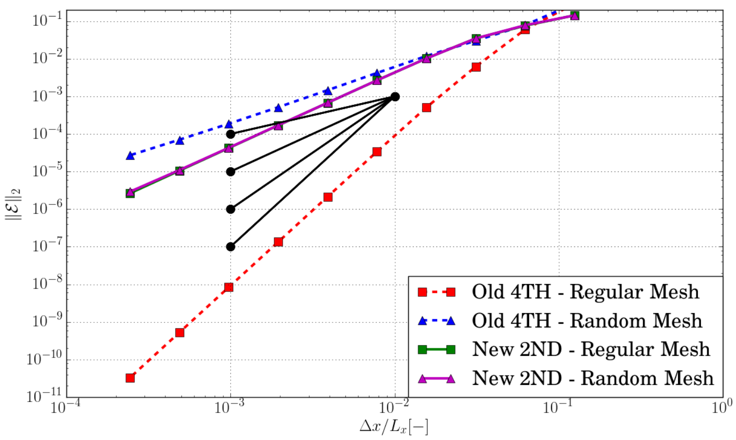

Figure 2: 3D - Spatial convergence for a bump function transported through a tri-periodic domain

degenerates to order 1.5 with the classical scheme.

Implementation of the new 3^{rd} order scheme is still in progress but the early results obtained with the new 2^{nd} order scheme are promising. For now, the scalar and its first and second derivatives are deconvoluted at the expected orders as presented in table 1. The next step is to ensure an accurate assembly of the residual by handling variation of the scalar on control-volume interfaces.

Mesh	Scalar	Gradient	Hessian
Regular	$\mathcal{O}(\Delta x^4)$	$\mathcal{O}(\Delta x^2)$	$\mathcal{O}(\Delta x^2)$
Shake	$\mathcal{O}(\Delta x^3)$	$\mathcal{O}(\Delta x^2)$	$\mathcal{O}(\Delta x^1)$

Table 1: Convergence order for 3^{rd} order data deconvolution in 3D